A Non-Newtonian liquid metal enabled enhanced electrography

Timosina, Veronika; Cole, Tim; Lu, Hongda; Shu, Jian; Zhou, Xiangbo; Zhang, Chengchen; Guo, Jinhong; Kavehei, Omid; Tang, Shi-Yang

DOI:
10.1016/j.bios.2023.115414

Biosensors and Bioelectronics 235 (2023) 115414

Contents lists available at ScienceDirect

Biosensors and Bioelectronics

journal homepage: www.elsevier.com/locate/bios

A Non-Newtonian liquid metal enabled enhanced electrography

Veronika Timosina [a], Tim Cole [a], Hongda Lu [b], Jian Shu [c], Xiangbo Zhou [c], Chengchen Zhang [d], Jinhong Guo [e], Omid Kavehei [f,g,**], Shi-Yang Tang [a,*]

[a] Department of Electronic, Electrical and Systems Engineering, University of Birmingham, Edgbaston, Birmingham, B15 2TT, UK
[b] School of Mechanical, Materials, Mechatronic, and Biomedical Engineering, University of Wollongong, Wollongong, Australia
[c] CAS Key Laboratory of Mechanical Behavior and Design of Materials, Department of Precision Machinery and Precision Instrumentation, University of Science and Technology of China, Hefei, China
[d] Graduate School of Biomedical Engineering, University of New South Wales, NSW, 2052, Australia
[e] The M.O.E. Key Laboratory of Laboratory Medical Diagnostics, The College of Laboratory Medicine, Chongqing Medical University, #1 Yixueyuan Road, Yuzhong District, Chongqing, 400016, China
[f] School of Biomedical Engineering, Faculty of Engineering, The University of Sydney, NSW, 2006, Australia
[g] The University of Sydney Nano Institute, Sydney, NSW, 2006, Australia

A B S T R A C T

Biopotential signals, like electrocardiography (ECG), electromyography (EMG), and electroencephalography (EEG), can help diagnose cardiological, musculoskeletal and neurological disorders. Dry silver/silver chloride (Ag/AgCl) electrodes are commonly used to obtain these signals. While a conductive hydrogel can be added to Ag/AgCl electrodes to improve the contact and adhesion between the electrode and the skin, dry electrodes are prone to movement. Considering that the conductive hydrogel dries over time, the use of these electrodes often creates an imbalanced skin-electrode impedance and a number of sensing issues in the front-end analogue circuit. This issue can be extended to several other electrode types that are commonly in use, in particular, for applications with a need for long-term wearable monitoring such as ambulatory epilepsy monitoring. Liquid metal alloys, such as eutectic gallium indium (EGaIn), can address key critical requirements around consistency and reliability but present challenges on low viscosity and the risk of leakage. To solve these problems, here, we demonstrate the use of a non-eutectic Ga–In alloy as a shear-thinning non-Newtonian fluid to offer superior performance to commercial hydrogel electrodes, dry electrodes, and conventional liquid metals for electrography measurements. This material has high viscosity when still and can flow like a liquid metal when sheared, preventing leakage while allowing the effective fabrication of electrodes. Moreover, the Ga–In alloy not only has good biocompatibility but also offers an outstanding skin-electrode interface, allowing for the long-term acquisition of high-quality biosignals. The presented Ga–In alloy is a superior alternative to conventional electrode materials for real-world electrography or bioimpedance measurement.

1. Introduction

Bioelectrodes are used to monitor body signals at the surface of the skin (Chen et al., 2021; Fang et al., 2021; Libanori et al., 2022; Meng et al. 2022a, 2022b; Zhao et al., 2021; Zhou et al., 2021). Electrodes non-invasively measure the biopotential arising from electrical activity by acting as transducers converting ionic current in the body into electric current for the measuring device. Such electrical activity can arise from muscle contraction in ECG and EMG, or localised electrical activity of neurons inside the brain in EEG. These electrographies can be used to analyse heart irregularities such as arrhythmia and neurological diseases such as epilepsy (Webster, 2009).

The most common electrodes used to record biosignals are Ag/AgCl electrodes due to their low cost and high signal quality (McAdams, 2006). Dry electrodes have non-conformable contact with skin which results in a high skin-electrode impedance, high signal noise, and high sensitivity to movements, leading to a decrease in the signal quality and reliability (Chi et al., 2010). A water-based electrolytic gel (hydrogel) can be added to Ag/AgCl electrodes to improve the contact between the electrode and the skin by creating conformal contact, which can decrease the impedance between the skin and the electrode by one order of magnitude (Li et al., 2017). However, the hydrogel is known to cause irritation due to the presence of chloride ions which function as ion charge carriers (Webster, 2009). During clinical long-term EEG monitoring, both types of electrodes cause discomfort. Dry electrodes require a headset to improve contact by adding pressure (e.g. spring-loaded electrodes), while wet electrodes require skin preparation involving skin abrasion to minimise impedance, which can cause further irritation

* Corresponding author.
** Corresponding author. School of Biomedical Engineering, Faculty of Engineering, The University of Sydney, NSW, 2006, Australia.
E-mail addresses: omid.kavehei@sydney.edu.au (O. Kavehei), S.Tang@bham.ac.uk (S.-Y. Tang).

https://doi.org/10.1016/j.bios.2023.115414
Received 9 February 2023; Received in revised form 17 May 2023; Accepted 19 May 2023
Available online 20 May 2023

and discomfort (Li et al., 2018; Shad et al., 2020). More importantly, hydrogel dries over time resulting in increased impedance and lack of suitability for long- and ultra-long-term monitoring. Therefore, the recording must be interrupted to clean the area and reapply the gel (Lin et al., 2010).

Gallium-based liquid metals, such as eutectic gallium-indium (EGaIn) and eutectic gallium-indium-tin (Galinstan), have recently become an attractive material in biomedical engineering where their uses have been explored in applications such as photothermal therapy for cancer treatment, X-ray and computerised tomography (CT) imaging, cardiac ultrasound imaging, and cochlear implants (Chechetka et al., 2017; Cole et al., 2021; Fan et al., 2020; Hu et al., 2023; Li et al., 2020; Strahl et al., 2016; Wang et al., 2020; Zhu et al., 2019). The increased attention is due to the material's appealing properties such as near-indefinite deformability, high electrical conductivity, high photo-thermal conversion efficiency, good biocompatibility, and antimicrobial functionality (Goss et al., 2018; Kim et al., 2018; Liu et al., 2011; Tang et al., 2021). Liquid metals have been previously used for biosignal monitoring. For example, Guo et al. created a wearable flexible electronic tattoo using Ni-EGaIn and polymethacrylate (PMA) glue (Guo et al., 2019). The tattoo could acquire ECG and EMG signals, showing comparable performance to conventional Ag/AgCl wet electrodes. Alberto et al. manufactured electronic tattoos using Ag–In-Ga and tattoo paper for electrophysiological monitoring (Alberto et al., 2020). The created ECG patches exhibited a better signal quality compared to Ag/AgCl wet electrodes and dry stainless-steel electrodes. Moreover, Lopes et al. used a similar method to fabricate Ag–In-Ga tattoo electrodes of which the performance was compared to seven different electrodes including Ag/AgCl wet electrodes for ECG and EMG recordings (Lopes et al., 2019).

While using PMA and tattoo paper could help adhere and peel off liquid metal to the skin, they also act as a thin insulating layer that has an impact on the conductivity of the electrode. Complex microfabrication processes are needed for electronic tattoos and the electrodes are often for one-time use only as the embedded liquid metal can hardly be separated from the adhesive materials. These factors compromise the cost-effectiveness of the device. Therefore, it is desirable to directly use liquid metal with minimum fabrication processes to facilitate the recycling of the material and reduce cost. As an electrode, liquid metal conforms to the surface of the skin without drying (due to liquid metal's extremely low vapour pressure) or irritating the skin, making it more appealing than hydrogel. The conformity and high electrical conductivity of the alloy decrease the impedance of the electrode and enable it to acquire a high-quality signal while being less prone to environmental noise such as power line noise. In addition, the amphoteric Ga oxide layer can be readily removed using either a strong base (such as sodium hydroxide (NaOH) solution) or a strong acid to induce the detachment and merging of liquid metal droplets for recycling (Tang et al., 2021). However, conventional liquid metals such as EGaIn have low viscosities (~2 times of water), which would risk the liquid metal leaking when adhering the electrode to the skin.

Here, we demonstrate the use of a non-eutectic Ga–In alloy (50 wt% Ga and 50 wt% In, $Ga_{50}In_{50}$) as a shear-thinning non-Newtonian fluid to offer superior performance to commercial hydrogel electrodes, dry electrodes, and conventional liquid metals for electrography measurements. We examine the biocompatibility of $Ga_{50}In_{50}$ and investigate the effectiveness of cleaning the alloy on the skin. The performance of the electrodes is evaluated using skin-electrode impedance and signal-to-noise ratio (SNR) from ECG, EEG, and EMG recordings as indicators of signal quality. The impedance of $Ga_{50}In_{50}$ and hydrogel is compared to observe how the impedance changes as the fluids are left to dry. Furthermore, we demonstrate that $Ga_{50}In_{50}$ is highly processable, allowing for the fabrication of electrodes with more complex configurations to further enhance signal SNR.

2. Materials and methods

2.1. Materials

Ga (99.99%) and Indium (99.995%) were purchased from Magnametals, UK. NaOH pellets were purchased from Sigma-Aldrich, UK. The copper tape (EMI Shielding Tape 1181) was purchased from 3M, UK. BioAmp EXG Pill kits were purchased from Crowd Supply, USA. RPMI 1640 medium and fetal bovine serum (FBS) were purchased from Gibco, Thermo Fisher Scientific, Australia. AlamarBlue was purchased from Bio-Rad, Australia. Cell Counting Kit 8 (CCK8) was purchased from Abcam, UK. Dulbecco's modified eagle's medium (DMEM, low glucose, Cat. No. 11885084) and l-glutamine (Cat. No. G7513) were purchased from Sigma-Aldrich, Australia. The wet facial wipes were purchased from Woolworths, Australia (brand: Simple Wipe, Unilever, UK), which contain ingredients of water, cetearyl isononanoate, benzoic acid, ceteareth-12, ceteareth-20, cetearyl alcohol, citric acid, dehydroacetic acid, disodium EDTA, glycerin, glyceryl stearate, panthenol, pantolactone, phenoxyethanol, sodium citrate, and tocopheryl acetate.

2.2. Cell culture and cytotoxicity tests

MEF feeder cells were cultured in DMEM containing 10% FBS and l-glutamine solution (2 mM) at 37 °C in an incubator containing 5% CO_2. MEF feeder cells (10^4/well) were seeded in 96-well plates for 24 h. The cytotoxicity of $Ga_{50}In_{50}$ was investigated in MEF feeder cells by CCK8.

4T1 cells were incubated in RPMI 1640 medium containing 10% FBS at 37 °C in a humidified atmosphere containing 5% CO_2. These cells were seeded in the 96-well plates at a density of 10^4 cells per well (100 μL) for 24 h. The cytotoxicity of $Ga_{50}In_{50}$ was investigated in 4T1 cells by alamarBlue assay.

2.3. Live/deal cell staining assay

MEF feeder and 4T1 cells were respectively seeded in 8-well plates at a density of 2×10^4 cells per well for 24 h $Ga_{50}In_{50}$ droplets were added into cells to further co-incubate for 24 h. After incubation, these cells were incubated with calcein-AM (2 μM) and ethidium homodimer (EthD-1, 4 μM) in PBS buffer solution at 37 °C for 30 min. After that, the cells were washed with phosphate buffered saline (PBS) 3 times and observed by a confocal microscope.

2.4. In-vivo experiment with mouse

All animal experiments were performed in accordance with the NIH Guide for the Care and Use of Laboratory Animals, after approval of the laboratory animal protocol by the Institutional Animal Care and Use Committee (IACUC) of the University of Science and Technology of China (Protocol Number USTCACUC23040123021). Adult mice (age: 5–6 weeks, sex: male, body weight: ~100 g) purchased from the First Affiliated Hospital of USTC were used in the study.

2.5. Electrode characterisation

Electrode impedance was measured using an impedance analyser (Agilent 4294 A) by applying a small alternating electrical current in a frequency range of 40 Hz to 10 MHz and measuring the response across two nodes. The test was performed at an ambient temperature of 24 °C and relative humidity of 51%. The skin-electrode impedance was measured three times for each electrode on a healthy volunteer. The rheology of $Ga_{50}In_{50}$, EGaIn, and hydrogel was characterised using a rheometer (Anton Paar MCR 302). The radius of the rotor plate was 9 mm, the gap between the plates was 0.15 mm, and the volume of liquid in the measuring gap was 0.25 mL. Temperature regulation was used to maintain the temperature at 33 °C. Shear stress vs. shear rate curves were obtained by varying the shear rate from 0.1 to 100 s^{-1}. Storage and

loss moduli were obtained by varying the oscillation frequency of the rotor plate from 0.1 to 30 Hz with a 1% shear amplitude.

The effectiveness of cleaning residual $Ga_{50}In_{50}$ on the skin was investigated by attaching the electrode to a pork belly for 24 h and measuring the concentration of Ga and In left on skin biopsy samples using an Agilent 7900 Inductively-Coupled Plasma Mass-Spectrometer (ICP-MS). Biopsy samples were taken using a 2 mm hole punch. The samples were then respectively placed in a 15 mL centrifuge tube containing 500 μL of hydrochloric acid (HCl) solution (1 mol/L). We sonicated the tubes in a sonication bath for 3 min and then added 10 mL of deionised (DI) water to make the final solution for the ICP-MS measurements.

2.6. Electrography measurements

BioAmp EXG Pill kits were used to acquire biopotential signals. The board uses a three-electrode differential electrode configuration meaning the recorded biopotential is the difference between two electrodes and a reference electrode. A data acquisition device with a 16-bit ADC (National Instruments DAQ USB-6002) was used to record ECG, EMG, and EEG signals. In this work, ECG was recorded on the ventral side of the wrists using an amplifier and an ADC converter. A wristband was placed on top of the electrodes to ensure optimum skin-electrode contact. Five 30-s ECG recordings were collected using hydrogel, $Ga_{50}In_{50}$, and dry Cu electrodes from a healthy volunteer. EEG was recorded from the frontal cortex positions Fp1 and Fp2 with reference placed on Fpz from the electrode system. A headband was placed on top of the electrodes to maximise contact with the skin. Five 30-s EEG recordings are made with each electrode type from a healthy volunteer. Separate recordings were made while the volunteer kept their eyes open and closed. The biopotential signals were recorded in Labview at a sampling frequency of 256 Hz to satisfy the Nyquist criterion as the frequency range of ECG and EEG is 0.01–100 Hz and 0–100 Hz, respectively (Li et al., 2010). To filter out power line noise, a 50 Hz and a 100 Hz notch filter were applied to the raw ECG and EEG data. The $Ga_{50}In_{50}$ and hydrogel electrodes were used to record two-channel surface EMG on the arm from 5 healthy volunteers. A 50 Hz and a 100 Hz notch filter are applied to remove power line noise. The SNR for recorded signals was calculated as SNR (dB) $= 20\log_{10}[(A_{raw} - A_{noise})/A_{raw}]$, where A_{raw} and A_{noise} are the amplitude of the recorded raw signal and the background noise, respectively.

3. Characterisation of $Ga_{50}In_{50}$ electrodes

3.1. Electrode preparation

Fig. 1a illustrates the process of producing $Ga_{50}In_{50}$. The alloy is prepared by dissolving In into liquid Ga at a 1-to-1 weight ratio at 200 °C. A paste is formed once the alloy is cooled. Fig. 1b demonstrates that $Ga_{50}In_{50}$ behaves like a solid and does not spill when turned upside down while EGaIn does. $Ga_{50}In_{50}$'s high viscosity at a steady state makes it easy to process, allowing the material to be manipulated using a spatula rather than a syringe (see Fig. 1b inset). As a paste, it adheres to Ag/AgCl and establishes satisfactory contact with the skin without spilling. In addition, the paste leaves minimal residue on the skin. Although a paste can be created by increasing the viscosity of EGaIn through a continuous oxidising process using a vortex mixer, it is difficult to control the level of oxidation in EGaIn to guarantee batch-to-batch (Yu et al., 2013). A more controlled method to increase the thickness of EGaIn is to increase the content of In as this will shift the phase of Ga–In away from the eutectic point and increase the melting point of the mixture.

Fig. 1c shows the fabrication process of the $Ga_{50}In_{50}$ electrode. The gel pad in a disposable Ag/AgCl electrode (Skintact) is removed and replaced with $Ga_{50}In_{50}$ paste. The electrode is then placed on the skin like the normal electrode. The hydrogel electrodes are prepared in a similar process using a conductive liquid hydrogel (SONOGEL Ultrasound Gel, Ana Wiz). The viscosity of the hydrogel is similar to liquid soap and therefore leaks when the electrode is applied to the skin. The dry copper electrode is fabricated by cutting the copper tape into a circle. The area of the electrode is kept the same for all different types of electrodes. Fig. 1d–f shows the hydrogel, $Ga_{50}In_{50}$, and dry copper electrodes and how they would interact with the skin surface. While the liquid nature of hydrogel and $Ga_{50}In_{50}$ allows them to fully conform to the epidermis, the copper electrode maintains insulating air gaps which compromise the signal quality (Fig. 1f).

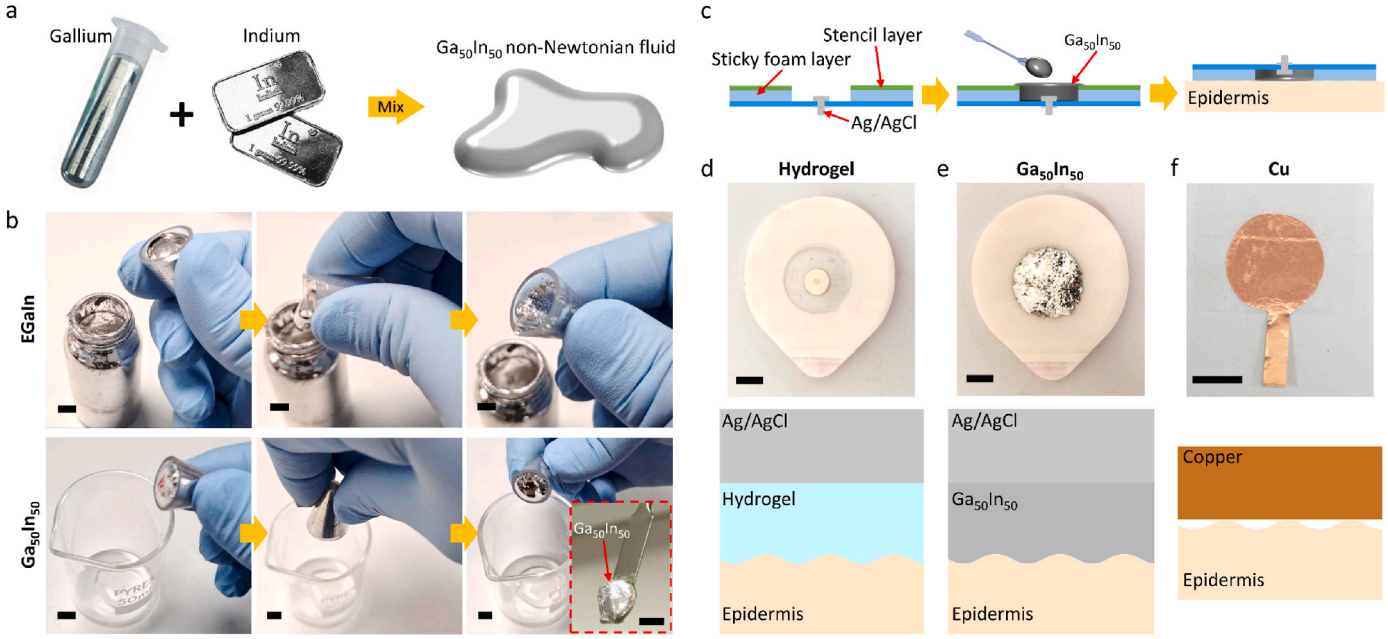

Fig. 1. Fabrication of electrodes. (a) Process of making $Ga_{50}In_{50}$. (b) Tilting EGaIn and $Ga_{50}In_{50}$ to show spillage. The inset shows that $Ga_{50}In_{50}$ can be transported using a spatula. (c) Schematics showing the process for making a $Ga_{50}In_{50}$ electrode. (d–f) Top view of hydrogel, $Ga_{50}In_{50}$ and copper electrode and how they would conform to interact with skin. Scale bars are 5 mm.

3.2. Biocompatibility tests of $Ga_{50}In_{50}$ electrodes

Long-term monitoring of electrograph signals requires the electrodes to be biocompatible without causing severe irritation or allergic reactions to the skin. We first conduct a skin irritation test by attaching a $Ga_{50}In_{50}$ electrode on one side of the mouse skin for a specific period, as shown in Fig. 2a. A standard hydrogel electrode (control) is attached to the other side for comparison. Similar to a hydrogel electrode, skin in contact with the $Ga_{50}In_{50}$ electrode exhibits no inflammation or irritation even after 3 days of attachment (Fig. 2b), indicating that $Ga_{50}In_{50}$ is biocompatible with skin.

We next evaluate the cytotoxicity of $Ga_{50}In_{50}$ using MEF feeder cells. In this test, cells are cultured for 24 h in a mixture of the culture medium and $Ga_{50}In_{50}$. Fig. 2c shows fluorescent images of MEF feeder cells with life/dead stains with and without the presence of $Ga_{50}In_{50}$, indicating very low cytotoxicity of $Ga_{50}In_{50}$. The inset of Fig. 2c shows the CCK8 assay results for the control and $Ga_{50}In_{50}$ groups, in which high cell viability above 85% is observed for both groups, further ensuring that $Ga_{50}In_{50}$ is biocompatible. We also evaluate the cytotoxicity of $Ga_{50}In_{50}$ using 4T1 breast cancer cells, as shown in Fig. S1, in which we can see high cell viability above 95%. Further investigation of $Ga_{50}In_{50}$ biocompatibility is necessary for future investigations. Co-culturing cells with $Ga_{50}In_{50}$ without direct touching cannot fully examine the material's biocompatibility. Mimicking the real-world scenario by testing the viability of skin tissues cultured directly on top of $Ga_{50}In_{50}$ would be more desirable. However, establishing an in-vitro tissue model that can fully mimic the complex structure of human skin is difficult, particularly the construction of the keratinocytes layer with the stratum corneum – the outermost layer of the skin with ~15–20 layers of dead cells (Menon et al., 2012). Such a layer acts as a barrier that prevents unwanted materials from entering. Moreover, the anti-inflammatory effect of Ga-based liquid metals (Zhang et al., 2022) may also impose significant effects on the long-term wearability of $Ga_{50}In_{50}$ electrodes, which is subject to further exploration.

After removing the $Ga_{50}In_{50}$ electrode, some residual material on the skin is observed. We investigated the effectiveness of cleaning residual material on the skin by attaching the electrode to a pork belly for 24 h and measuring Ga and In concentrations in biopsy samples using ICP-MS. Fig. 2d shows the surface of the pork belly sample right after removing the electrode (W0) and wiping the surface gently with wet skin cleansing facial wipes four times (W1–W4). Two times wiping is sufficient to remove most of the residual materials and no damage to the sample skin is observed after repetitive wiping. A biopsy sample is taken after each wipe (denoted as S1–S4). The red circle indicated the position of the $Ga_{50}In_{50}$ electrode before detachment. The ICP-MS measurements for solutions containing biopsy samples (see Electrode characterisation section) indicate that three times wiping is sufficient to remove most of the residual, as shown in Fig. 2e. Directly washing the skin using liquid soap (Dettol Hand Wash) for 3 min without wiping can also effectively remove the residual materials (see "Liquid soap" row in Fig. 2e). The most effective approach is to wipe the skin three times first and then clean it with liquid soap for 3 min (see "Wipe + liquid soap" row in Fig. 2e).

3.3. Rheological properties

We characterised the rheological properties of $Ga_{50}In_{50}$, EGaIn liquid metal, and hydrogel, as shown in Fig. 3a and Fig. S2. The viscosity vs. shear rate plots presented in Fig. 3a indicate that all materials exhibit non-Newtonian behaviour and shear-thinning tendencies (see Fig. S2a for the shear stress vs. shear rate plots). The viscosity of $Ga_{50}In_{50}$ is exceptionally high (~30,000 Pa s), which is two orders of magnitude greater than that of EGaIn and hydrogel at low shear rates. At 33 °C, $Ga_{50}In_{50}$ is biphasic, composed of solid In particles suspended in liquid metal, making it granular and highly viscous when at rest (Anderson and Ansara, 1991). The presence of suspended In particles in the granular

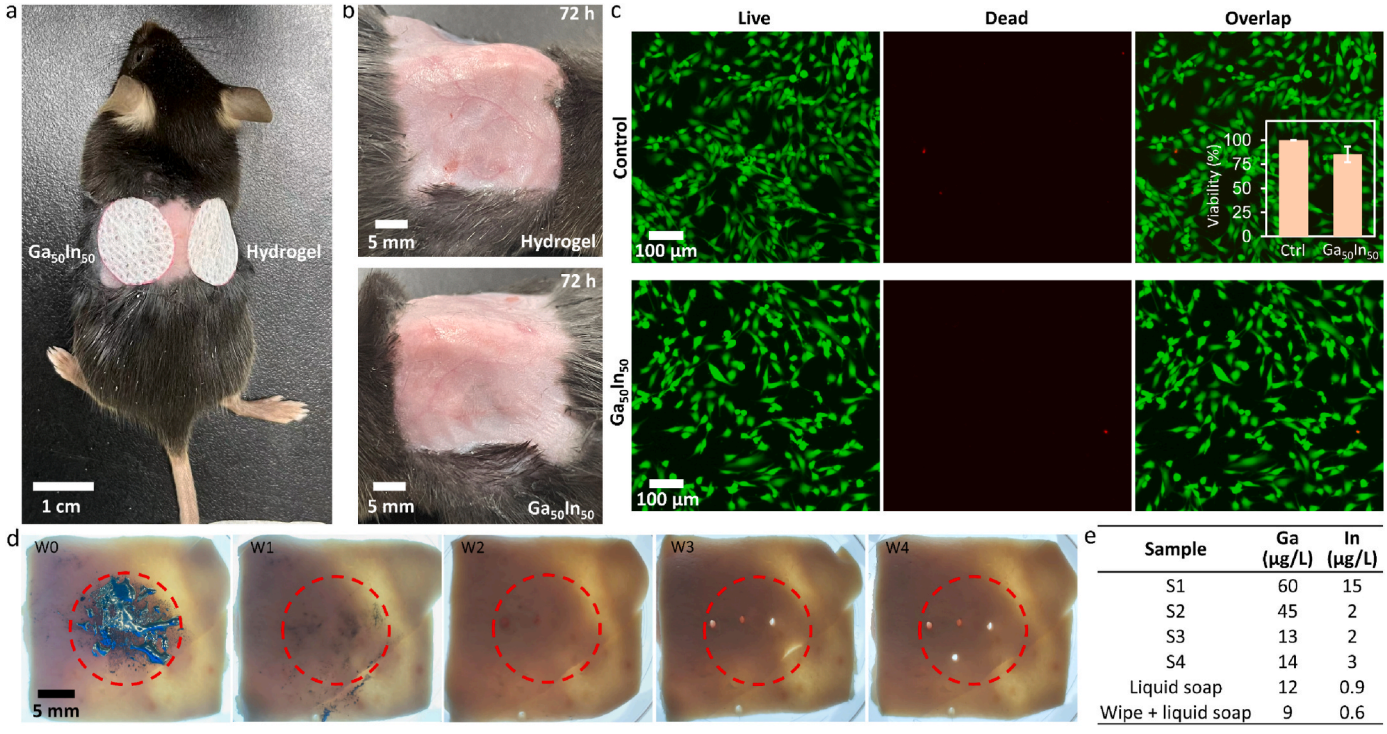

e

Sample	Ga (µg/L)	In (µg/L)
S1	60	15
S2	45	2
S3	13	2
S4	14	3
Liquid soap	12	0.9
Wipe + liquid soap	9	0.6

Fig. 2. Biocompatibility test of $Ga_{50}In_{50}$ electrodes. (a) Skin irritation test with the $Ga_{50}In_{50}$ electrode and a standard hydrogel electrode on a mouse. (b) Images of the mouse skin after 3 days of electrode attachment. (c) Fluorescent images of MEF feeder cells stained with calcein-AM and EthD-1 after 24 h of incubation with and without $Ga_{50}In_{50}$ (control). The inset shows the CCK8 assay results. (d) Images of a pork belly skin after removing the $Ga_{50}In_{50}$ electrode (W0) and cleaning the surface using a cleansing wipe for 1–4 times (W1–W4). A biopsy sample is taken after each wipe. (e) Table showing the concentration of Ga and In residuals after wiping and washing with liquid soap.

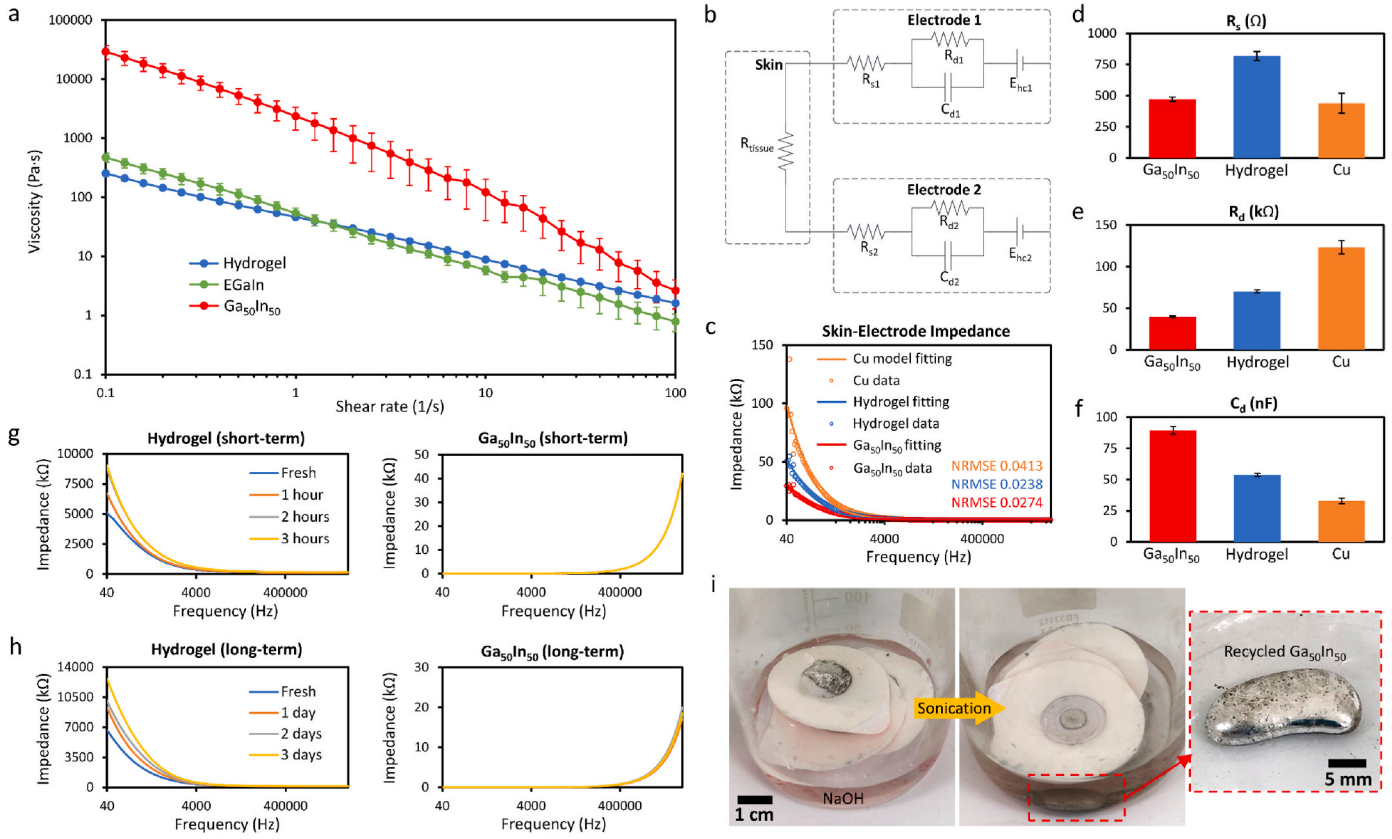

Fig. 3. Characterisation of electrodes. (a) Viscosity vs shear rate plots for hydrogel, EGaIn, and $Ga_{50}In_{50}$. (b) Skin-electrode interface equivalent circuit. (c) Frequency vs impedance data and fitting curves for copper, hydrogel, and $Ga_{50}In_{50}$ electrodes. Comparison of (d) series resistance R_s, (e) interface resistance R_d, and (f) interface capacitance C_d for $Ga_{50}In_{50}$, hydrogel, and copper electrodes. Frequency vs impedance curves for (g) short-term (3 h) and (h) long-term (3 days) experiments for hydrogel and $Ga_{50}In_{50}$ electrodes. (i) Processes of recycling $Ga_{50}In_{50}$ material.

$Ga_{50}In_{50}$ mixture leads to a jamming effect, resulting in a paste-like consistency at the steady state. However, by stirring the material, the In particles can be effectively separated, leading to a reduction in viscosity (also the shear stress). This behaviour resembles that of EGaIn pastes containing a significant proportion of silicone particles (>85 wt %), which also exhibit a noticeable decrease in shear stress at higher shear rates (Chang et al., 2020).

At a higher shear rate of 100 s^{-1}, the viscosity of $Ga_{50}In_{50}$ decreases significantly by over 10,000 times to levels similar to those of EGaIn and hydrogel. The significant change in viscosity of $Ga_{50}In_{50}$ is further illustrated in Movie S1, in which we can see that $Ga_{50}In_{50}$ behaves more like a solid, unlike EGaIn, when shaken. However, stirring the material makes $Ga_{50}In_{50}$ behave more like a liquid (see Movie S1). This unique property allows $Ga_{50}In_{50}$ to be reshaped at a high shear rate and remain stable as a solid material at low shear rates. We found that increasing the content of In the Ga–In alloy makes the material more viscous at both low and high shear rates (see Fig. S2b). The storage and loss modulus measurements for $Ga_{50}In_{50}$, EGaIn, and hydrogel at various frequencies are given in Figs. S2c–d. For $Ga_{50}In_{50}$, increasing the oscillation frequency (i.e., the shear rate) leads to a decrease in the storage modulus, which further indicates that $Ga_{50}In_{50}$ is shear-thinning.

Supplementary videos related to this article can be found at https://doi.org/10.1016/j.bios.2023.115414

To further demonstrate the stability of $Ga_{50}In_{50}$, we placed the material on a stretchable Ecoflex elastomeric substrate that simulates the physical properties of human skin and applied large strains repeatedly, as shown in Movie S2. $Ga_{50}In_{50}$ can stick to the substrate without flowing. These properties benefit the use of $Ga_{50}In_{50}$ for making wearable electrodes – the low viscosity at a high shear rate implies that the alloy can be reshaped by mixing to allow it to be filled into the cavity of a disposable Ag/AgCl electrode simply using a spatula (see Movie S1 and Fig. 1b). Also, the semi-fluidic property of $Ga_{50}In_{50}$ allows it to conform to the skin surface to maximise the contact area. Moreover, the high viscosity of $Ga_{50}In_{50}$ at a low shear rate makes the alloy capable of keeping its shape without leaking when the electrode is placed on the skin. On the contrary, the low viscosity of hydrogel and EGaIn makes them more prone to leaking.

Supplementary videos related to this article can be found at https://doi.org/10.1016/j.bios.2023.115414

3.4. Skin-electrode impedance measurements

Skin-electrode impedance is an accurate indicator of the signal quality of bioelectrodes as it determines the ease of obtaining a biological signal from the body (Lopes et al., 2019; Mathewson et al., 2017). Impedance was measured by applying a small AC electrical current in a frequency range of 40 Hz–100 kHz across two nodes. The electrodes are placed on the ventral side of the forearm, distanced 40 mm between the centres of the electrodes. The impedance of one electrode is determined by halving the total impedance (Yang et al., 2018). The skin is cleaned with soap and water after removing each electrode. The skin-electrode interface is essentially modelled by the equivalent circuit shown in Fig. 3b, and the equivalent impedance Z_e is expressed as (Albulbul, 2016):

$$Z_e = R_s + \frac{R_d}{1 + j2\pi f C_d R_d} \quad (1)$$

where R_s is series resistance, R_d is interface resistance, C_d is interface capacitance, and f is signal frequency. R_s represents the ease of movement between the electrodes at the surface of the skin combined with the

resistance of the electrode material. The electrode (Ag/AgCl and copper) and skin act as two capacitive plates with conductive gel, liquid metal, or air in between them. R_d and C_d represent the resistance of charge movement between skin and electrode, and capacitance originated from the moving charges between the electrode-skin double layer (Lopes et al., 2019). In the equivalent circuit, R_{tissue} is small and considered negligible and is therefore not included in the function (Albulbul, 2016). To minimise the impedance Z_e, R_s and R_d should be low, and C_d should be high. The parameters R_s, R_d and C_d are estimated by fitting the skin-electrode impedance data to Equation (1) using the Python package (Murbach et al., 2020). The package uses the Basin-hopping global optimisation algorithm instead of the common impedance model fitting method non-linear least squares regression as it is less sensitive to initial values that may increase the error between the measured data and the model. The normalised root-mean-square error (NRMSE) was estimated for each model.

Fig. 3c shows the skin-electrode impedance measurement and fitted model of each electrode. $Ga_{50}In_{50}$ has an impedance of approximately 30 kΩ suggesting superior skin-electrode contact to copper and hydrogel electrodes which exhibit higher impedances of approximately 50 kΩ and 97 kΩ, respectively. The estimations of the equivalent circuit parameters for each electrode are shown in Fig. 3d–f. As the value of R_s is related to the resistance of the material, $Ga_{50}In_{50}$ and Cu electrodes have low R_s values compared to conductive hydrogel due to their high electrical conductivity (Fig. 3d). R_d and C_d are related to the charge flow between the skin and the electrode. $Ga_{50}In_{50}$ has the lowest R_d and the highest C_d due to its prominent level of conformity and high electrical conductivity (Fig. 3e and f). While the hydrogel wets and fully conforms to the skin due to its low surface tension and viscosity, it is less conductive compared to $Ga_{50}In_{50}$ and Cu. The Cu electrode has the highest R_d and the lowest C_d as it does not conform to the skin, despite copper being a good electrical conductor (Fig. 3e and f). The capacitance of an electrode is directly proportional to its surface area. When an electrode conforms to the skin, it utilises its entire surface area, resulting in maximum capacitance. However, if the electrode does not conform to the skin, there may be gaps of air between the electrode and the skin, which limits the effective contact area and, therefore, reduces the capacitance (Lopes et al., 2019). The area of the Cu electrode that interfaces with the skin is less than the hydrogel and $Ga_{50}In_{50}$ electrodes due to the existence of an air gap in the cavities of the skin. The $Ga_{50}In_{50}$ electrode's low R_s and R_d and high C_d suggest that it has the potential to offer better signal conduction performance from the skin, thus giving the highest signal quality out of the three electrodes.

3.5. Short and long-term impedance tests

Once hydrogel has been applied to the electrode, it begins to evaporate due to its high water content (Mathewson et al., 2017). This reduces the mobility of chloride ions thus increasing the impedance of the electrode. Ga-based liquid metals, however, have negligible vapour pressure and therefore do not evaporate. To examine the stability of impedance over time, hydrogel and $Ga_{50}In_{50}$ are each placed in a polylactic acid (PLA) hollow cuboid on a Cu tape for measuring impedance over a frequency range from 40 Hz to 10 MHz. Such a test is conducted without covering the cuboids for 3 h to observe how the fluids evaporate in the open air. When recording EEG, electrodes are exposed to air therefore this short-term test would represent the impedance change of such a setting. Another test is done where the fluids are covered with PLA leads and measured every 24 h for four days. The test is performed in a sealed box to keep the test environment constant. This test represents how the impedance changes when the electrodes are not exposed to air for ECG or EMG recordings.

Fig. 3g and h shows the results of the short-term and long-term impedance tests, respectively. In the short-term test, the hydrogel has an impedance of 5.1 kΩ when freshly applied to the cuboid. After only 3 h, the impedance increases to 10.7 kΩ. Meanwhile, the impedance of $Ga_{50}In_{50}$ starts at approximately 0.05 kΩ and remains the same 3 h later. Despite covering the fluid in the long-term test, the impedance of the hydrogel increases over time. The lid does not fully isolate the conductive gel therefore some of it will still evaporate. The impedance of $Ga_{50}In_{50}$ remains unchanged. The increase in impedance for the case of $Ga_{50}In_{50}$ at high frequencies is likely due to the skin effect. This effect causes AC high-frequency currents to concentrate near the surface of a conducting material, reducing the effective cross-sectional area available for current flow and increasing the resistance of the conductor. The short-term and long-term impedance results suggest that $Ga_{50}In_{50}$ has an advantage over hydrogel as it does not evaporate, and the impedance would stay constant throughout electrographic recordings. For long-term EEG recordings, using $Ga_{50}In_{50}$ would eliminate the need to stop the recording to clean up or reapply the fluid which is the case with hydrogel.

$Ga_{50}In_{50}$ can be recycled after usage, as shown in Fig. 3i. Used electrodes are collected in a flask filled with NaOH solution (0.5 mol/L) and then sonicated in a sonication bath for 5 min. The metal separates from the electrodes and combines into a large droplet at the bottom of the beaker. The $Ga_{50}In_{50}$ metal is collected and washed with DI water for reuse. The recyclability of $Ga_{50}In_{50}$ poses an advantage to the hydrogel.

4. Electrography measurements

Fig. 4a shows a 5-s segment of the raw ECG signal collected by Cu, hydrogel, and $Ga_{50}In_{50}$ electrodes. ECG has a distinctive signal pattern that partly consists of a QRS complex which signifies the depolarisation of ventricular muscle cells observed as a decline (Q) followed by a peak (R) followed by a decline (S) (Lilly, 2012). The dry Cu electrode is slightly noisier compared to other electrodes. Fig. 4b compares the average SNR from five 30-s ECG readings of each type of electrode. The Cu electrode has the lowest average SNR at 23.5 dB. Both the $Ga_{50}In_{50}$ and the hydrogel electrodes have higher average SNRs of approximately 27.7 dB and 27.1 dB, respectively. The SNR suggest that $Ga_{50}In_{50}$ and hydrogel electrodes have similar ECG signal quality. The hydrogel electrode has the smallest standard error which suggests that the signal that the electrode records is more consistent. The skin on the wrist is relatively smooth therefore good skin-electrode contact can be established, even with dry Cu electrodes. Our study includes an evaluation of the performance of recycled $Ga_{50}In_{50}$ electrodes for ECG measurements. Our findings indicate that there is no noticeable difference between the performance of freshly prepared and recycled $Ga_{50}In_{50}$, as illustrated in Fig. S3. On the other hand, when the human subject moved during the measurement, the ECG signals recorded displayed notable distortion, as depicted in Fig. S4.

Unlike stationary ECG signal, EEG is generally a nonstationary signal and does not have a distinctive signal pattern while it can be considered distinctive to a degree if it is recorded in short time-windows and in response to a specific stimulus. EEG signal is analysed by its decomposition into frequency bands, each represents a state of the brain or brain waves (Sanei and Chambers, 2021). Comparing different types of EEG electrodes can be challenging as ideal comparisons require evaluation at the same location and time. To reduce errors, we keep electrodes in the same location while measuring a repeatable movement, such as opening and closing the eyes. From open-eye EEG, eye blinks can be observed. Fig. 4c and e respectively show a 10-s segment from the raw open-eye and closed-eye EEG data collected from different types of electrodes. The $Ga_{50}In_{50}$ electrode appears to have the least noise compared to other electrodes (Fig. 4d and f). The SNR results show that the $Ga_{50}In_{50}$ electrode has the highest SNR while the copper electrode has the lowest. The skin on the forehead is less smooth than the wrist skin therefore it was difficult for the dry electrode to establish good skin contact. Together with the skin-electrode impedance results, $Ga_{50}In_{50}$ shows to be an excellent replacement for hydrogel.

The $Ga_{50}In_{50}$ and hydrogel electrodes are used to record two-channel surface EMG on the arm in an attempt to classify the opening and closing

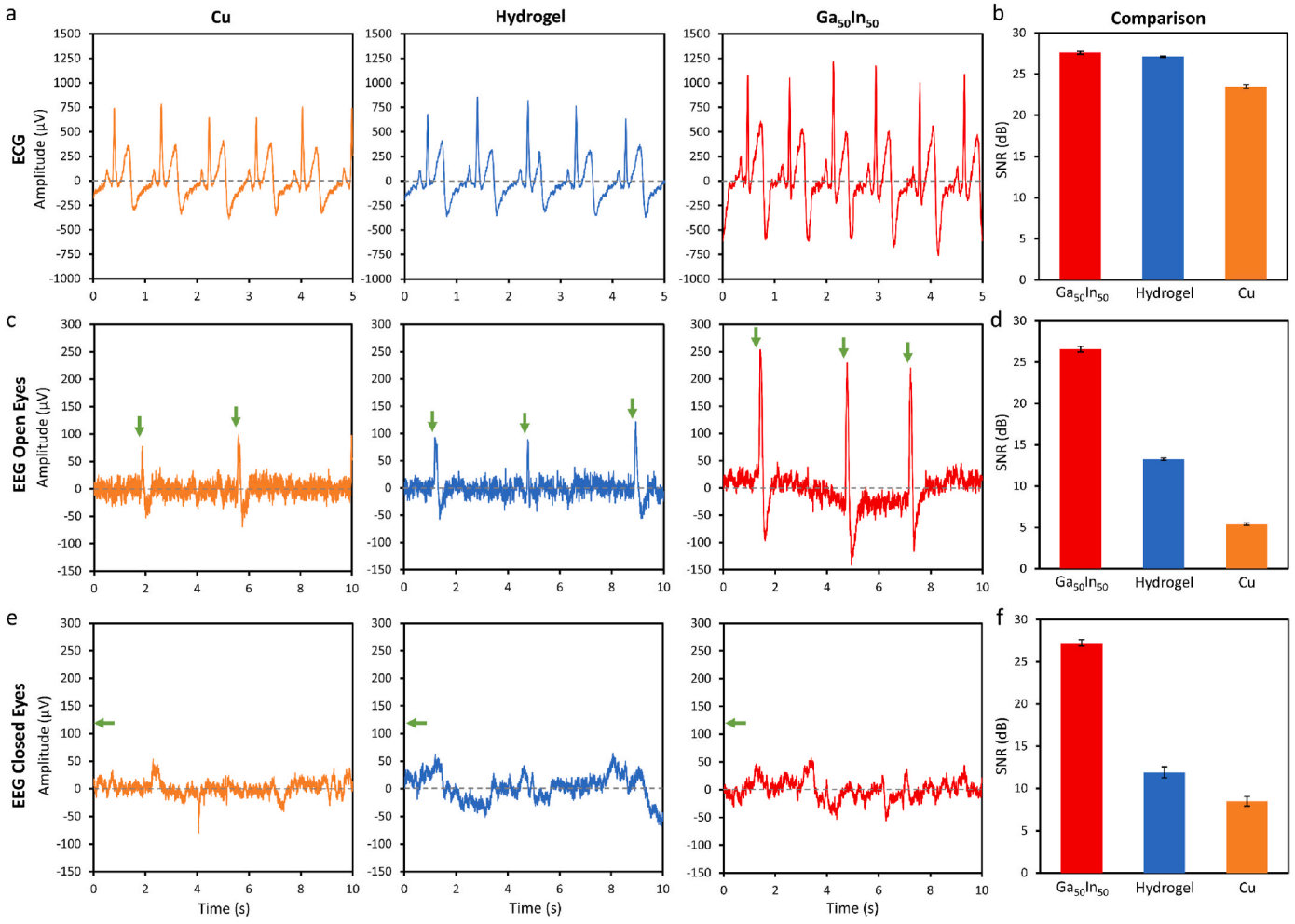

Fig. 4. ECG and EEG measurements. Recorded signal segments and SNR of (a–b) ECG, (c–d) EEG for open eyes, and (e–f) EEG for closed eyes obtained by Cu, hydrogel, and $Ga_{50}In_{50}$ electrodes. The green arrows in (c) indicate the moment when eyes are open, while the green arrows in (e) indicate that eyes are closed from 0 s.

of the hand. A dataset containing one hundred 5-s EMG recordings for each hand gesture from 5 healthy volunteers is created. A 50 Hz and a 100 Hz notch filter are applied to remove power line noise. Fig. 5a–d shows the EMG signals acquired by $Ga_{50}In_{50}$ and hydrogel electrodes from open and closed hand gestures. We record signals from two channels located at different places on the arm (see inset of Fig. 5a). Signals acquired by $Ga_{50}In_{50}$ electrodes show a more apparent difference between the hand gestures. Fig. 5e and f show the average SNR of each channel and electrode. While the $Ga_{50}In_{50}$ electrode has a higher SNR than hydrogel, the standard error is bigger.

In addition, we explore the application of machine learning for hand gesture recognition when using $Ga_{50}In_{50}$ and hydrogel as electrodes. To generate training data, EMG signals are recorded using these two types of electrodes from 5 individuals at a 512 Hz sampling rate using two channels. Each recording is 5 s long and consists of the muscle activity when the individual opens or closes their hand. The collected data is labelled as "open" or "close" to indicate the corresponding muscle activity. 100 recordings are collected from open and close hand movements, respectively. Thus, 1000 recordings are collected in total per channel. We remove 1 s of data from the beginning and end of each recording, making one recording 3 s long. The data is divided into 29 segments which are 200 ms long and overlap by 100 ms (each segment contains ~100 data). For each segment, 17 time-domain features are extracted (Abbaspour et al., 2020). Principal Component Analysis (PCA) is used to reduce the dimensionality of the dataset and identify the three most significant features, transforming each 17-dimensional feature vector into a 3-dimensional feature vector that will constitute the input to the bilayer artificial neural network (10 neurons in a hidden layer) with the rectified linear unit (ReLU) activation. We split the PCA processed data into training, validation, and testing sets. The data is then used to train a bilayer neural network to classify the hand gestures labelled "open" and "close" as the outputs (Fig. 5g). The classification accuracy is 67% for $Ga_{50}In_{50}$ electrodes and 65% for hydrogel electrodes. Our experiments indicate that $Ga_{50}In_{50}$ electrodes do not offer a significant advantage over hydrogel electrodes for hand gesture recognition, possibly due to the suboptimum neural network. Nonetheless, considering the high SNR of $Ga_{50}In_{50}$ electrodes and their other benefits, we can conclude that $Ga_{50}In_{50}$ is a viable alternative to hydrogel for EMG applications.

It is essential to highlight that machine learning classification is not the point of this article but necessary to present a complete picture of the capabilities our innovation on the quality signal recording offers. Therefore, this publication does not aim to enhance or improve cutting-edge achievements in classification. We believe higher quality recording will result in more meaningful biomarker discovery and classification, which is the subject of ongoing research in our research teams.

Bipolar electrodes are known to increase the spatial resolution of EMG signals (Disselhorst-Klug et al., 1997). The excellent processability of $Ga_{50}In_{50}$ allows us to readily fabricate bipolar electrodes to measure single-channel surface EMG, as shown in Fig. 5h. This can also extend to

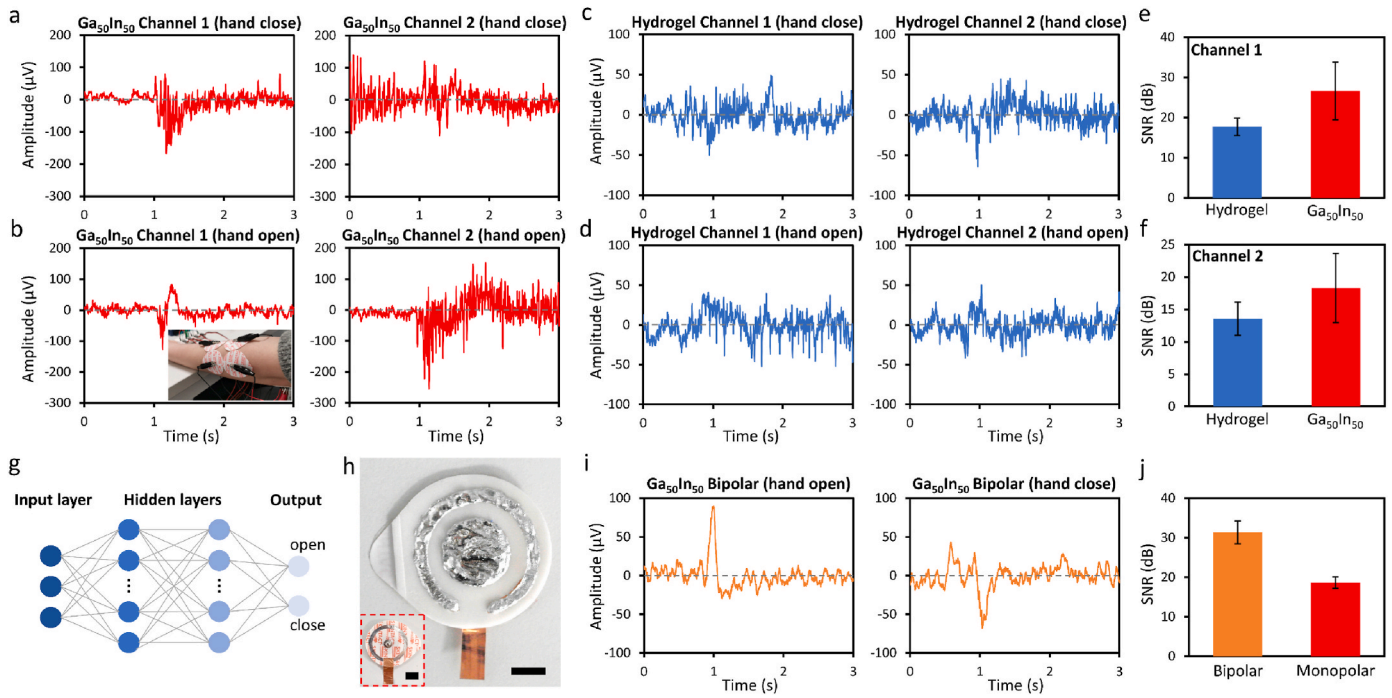

Fig. 5. EMG measurements using $Ga_{50}In_{50}$ and hydrogel electrodes. Three second segments of open and close hand gestures obtained by (a–b) $Ga_{50}In_{50}$ and (c–d) hydrogel electrodes from two channels. (e–f) Comparison of SNR of hydrogel and $Ga_{50}In_{50}$ electrodes for both channels. (g) Structure of the bilayer neural network used for signal classification. (h) Top view of a $Ga_{50}In_{50}$ bipolar electrode. The inset shows the bottom side of the bipolar electrode. The Cu tape is connected to the outer ring electrode. Scale bars are 5 mm. (i) Three-second segments of open and closed-hand gestures obtained by the bipolar $Ga_{50}In_{50}$ electrode. (j) Comparison of SNR of bipolar and monopolar $Ga_{50}In_{50}$ electrodes.

tripolar electrodes that allow a more dominant Laplacian EEG with a higher degree of reduction in confounding signals (Nasrollaholhosseini et al., 2019). A 3-s segment of the signal measured by bipolar electrodes is shown in Fig. 5i. Fig. 5j shows the comparison of SNR between the bipolar and the previously used monopolar electrodes. The bipolar electrode has a much higher SNR than the monopolar one, suggesting a higher signal quality.

5. Conclusion

In this study, we developed a non-Newtonian conductive fluid composed of 50 wt% Ga and 50 wt% In ($Ga_{50}In_{50}$) for making electrographic electrodes that can offer superior performance for the acquisition of biosignals compared to dry Cu and hydrogel electrodes. $Ga_{50}In_{50}$ exhibit a shear-thinning rheological property, which has a very high viscosity when placed steady and can behave like a normal liquid metal when exerting a high shear rate. Such a unique property makes the material highly processable that can be reconfigured to complex shapes, while preventing leakage when electrodes are formed, which cannot be achieved using conventional liquid metal or hydrogel. More importantly, the high conductivity and fluidic properties of $Ga_{50}In_{50}$ offer an outstanding skin-electrode interface, allowing for acquiring signals with high SNRs. Compared to hydrogel, the extremely low vapour pressure of $Ga_{50}In_{50}$ prevents evaporation, making the long-term monitoring of biosignals possible without signal decay and the need for replacing the materials. Moreover, $Ga_{50}In_{50}$ is recyclable and exhibits good biocompatibility without causing skin irritation or allergic reactions. We examined the advantages of $Ga_{50}In_{50}$ by making electrodes for ECG, EMG, and EEG measurements, indicating that $Ga_{50}In_{50}$ is a promising alternative to dry metal, wet hydrogel, and normal liquid metal electrodes.

CRediT authorship contribution statement

Veronika Timosina: Methodology, Data curation, Formal analysis, Writing – original draft. **Tim Cole:** Data curation, Investigation, Validation. **Hongda Lu:** Data curation, Investigation. **Jian Shu:** Data curation, Investigation, Resources. **Xiangbo Zhou:** Data curation, Investigation. **Chengchen Zhang:** Data curation, Investigation, Resources. **Jinhong Guo:** Data curation, Investigation, Visualization. **Omid Kavehei:** Conceptualization, Supervision, Visualization, Writing – review & editing. **Shi-Yang Tang:** Conceptualization, Resources, Supervision, Investigation, Project administration, Writing – review & editing.

Declaration of competing interest

The authors declare that they have no known competing financial interests or personal relationships that could have appeared to influence the work reported in this paper. Omid Kavehei is the founder and current Director of BrainConnect Pty Ltd.

Data availability

Data will be made available on request.

Acknowledgements

This work was funded by Engineering and Physical Sciences Research Council (EPSRC) grant EP/V008382/1 and the Australian Research Council Discovery Project grant DP230100019.

Appendix ASupplementary data

Supplementary data to this article can be found online at https://doi.org/10.1016/j.bios.2023.115414.

References

Abbaspour, S., Lindén, M., Gholamhosseini, H., Naber, A., Ortiz-Catalan, M., 2020. Evaluation of surface EMG-based recognition algorithms for decoding hand movements. Med. Biol. Eng. Comput. 58, 83–100.

Alberto, J., Leal, C., Fernandes, C., Lopes, P.A., Paisana, H., de Almeida, A.T., Tavakoli, M., 2020. Fully untethered battery-free biomonitoring electronic tattoo with wireless energy harvesting. Sci. Rep. 10 (1), 5539.

Albulbul, A., 2016. Evaluating major electrode types for idle biological signal measurements for modern medical technology. Bioengineering 3 (3), 20.

Anderson, T., Ansara, I., 1991. The Ga-In (gallium-indium) system. J. Phase Equil. 12, 64–72.

Chang, H., Zhang, P., Guo, R., Cui, Y., Hou, Y., Sun, Z., Rao, W., 2020. Recoverable liquid metal paste with reversible rheological characteristic for electronics printing. ACS Appl. Mater. Interfaces 12 (12), 14125–14135.

Chechetka, S.A., Yu, Y., Zhen, X., Pramanik, M., Pu, K., Miyako, E., 2017. Light-driven liquid metal nanotransformers for biomedical theranostics. Nat. Commun. 8 (1), 15432.

Chen, G., Xiao, X., Zhao, X., Tat, T., Bick, M., Chen, J., 2021. Electronic textiles for wearable point-of-care systems. Chem. Rev. 122 (3), 3259–3291.

Chi, Y.M., Jung, T.-P., Cauwenberghs, G., 2010. Dry-contact and noncontact biopotential electrodes: methodological review. IEEE Reviews in Biomedical Engineering 3, 106–119.

Cole, T., Khoshmanesh, K., Tang, S.-Y., 2021. Liquid metal enabled biodevices. Advanced Intelligent Systems 3 (7), 2000275.

Disselhorst-Klug, C., Silny, J., Rau, G., 1997. Improvement of spatial resolution in surface-EMG: a theoretical and experimental comparison of different spatial filters. IEEE (Inst. Electr. Electron. Eng.) Trans. Biomed. Eng. 44 (7), 567–574.

Fan, L., Duan, M., Sun, X., Wang, H., Liu, J., 2020. Injectable liquid metal-and methotrexate-loaded microsphere for cancer chemophotothermal synergistic therapy. ACS Appl. Bio Mater. 3 (6), 3553–3559.

Fang, Y., Zou, Y., Xu, J., Chen, G., Zhou, Y., Deng, W., Zhao, X., Roustaei, M., Hsiai, T.K., Chen, J., 2021. Ambulatory cardiovascular monitoring via a machine-learning-assisted textile triboelectric sensor. Adv. Mater. 33 (41), 2104178.

Goss, C.H., Kaneko, Y., Khuu, L., Anderson, G.D., Ravishankar, S., Aitken, M.L., Lechtzin, N., Zhou, G., Czyz, D.M., McLean, K., 2018. Gallium disrupts bacterial iron metabolism and has therapeutic effects in mice and humans with lung infections. Sci. Transl. Med. 10 (460), eaat7520.

Guo, R., Sun, X., Yao, S., Duan, M., Wang, H., Liu, J., Deng, Z., 2019. Semi-Liquid-Metal-(Ni-EGaIn)-Based ultraconformable electronic tattoo. Advanced Materials Technologies 4 (8), 1900183.

Hu, H., Huang, H., Li, M., Gao, X., Yin, L., Qi, R., Wu, R.S., Chen, X., Ma, Y., Shi, K., 2023. A wearable cardiac ultrasound imager. Nature 613 (7945), 667–675.

Kim, J.-H., Kim, S., So, J.-H., Kim, K., Koo, H.-J., 2018. Cytotoxicity of gallium–indium liquid metal in an aqueous environment. ACS Appl. Mater. Interfaces 10 (20), 17448–17454.

Li, G., Wang, S., Duan, Y.Y., 2017. Towards gel-free electrodes: a systematic study of electrode-skin impedance. Sensor. Actuator. B Chem. 241, 1244–1255.

Li, G., Wang, S., Duan, Y.Y., 2018. Towards conductive-gel-free electrodes: understanding the wet electrode, semi-dry electrode and dry electrode-skin interface impedance using electrochemical impedance spectroscopy fitting. Sensor. Actuator. B Chem. 277, 250–260.

Li, H., Qiao, R., Davis, T.P., Tang, S.-Y., 2020. Biomedical applications of liquid metal nanoparticles: a critical review. Biosensors 10 (12), 196.

Li, Y., Poon, C.C., Zhang, Y.-T., 2010. Analog integrated circuits design for processing physiological signals. IEEE Reviews in Biomedical Engineering 3, 93–105.

Libanori, A., Chen, G., Zhao, X., Zhou, Y., Chen, J., 2022. Smart textiles for personalized healthcare. Nature Electronics 5 (3), 142–156.

Lilly, L.S., 2012. Pathophysiology of Heart Disease: a Collaborative Project of Medical Students and Faculty. Lippincott Williams & Wilkins.

Lin, C.-T., Liao, L.-D., Liu, Y.-H., Wang, I.-J., Lin, B.-S., Chang, J.-Y., 2010. Novel dry polymer foam electrodes for long-term EEG measurement. IEEE (Inst. Electr. Electron. Eng.) Trans. Biomed. Eng. 58 (5), 1200–1207.

Liu, T., Sen, P., Kim, C.-J., 2011. Characterization of nontoxic liquid-metal alloy galinstan for applications in microdevices. J. Microelectromech. Syst. 21 (2), 443–450.

Lopes, P.A., Vaz Gomes, D., Green Marques, D., Faia, P., Góis, J., Patrício, T.F., Coelho, J., Serra, A., de Almeida, A.T., Majidi, C., 2019. Soft bioelectronic stickers: selection and evaluation of skin-interfacing electrodes. Advanced Healthcare Materials 8 (15), 1900234.

Mathewson, K.E., Harrison, T.J., Kizuk, S.A., 2017. High and dry? Comparing active dry EEG electrodes to active and passive wet electrodes. Psychophysiology 54 (1), 74–82.

McAdams, E., 2006. Bioelectrodes. Encyclopedia of Medical Devices and Instrumentation.

Meng, K., Xiao, X., Liu, Z., Shen, S., Tat, T., Wang, Z., Lu, C., Ding, W., He, X., Yang, J., 2022a. Kirigami-inspired pressure sensors for wearable dynamic cardiovascular monitoring. Adv. Mater. 34 (36), 2202478.

Meng, K., Xiao, X., Wei, W., Chen, G., Nashalian, A., Shen, S., Xiao, X., Chen, J., 2022b. Wearable pressure sensors for pulse wave monitoring. Adv. Mater. 34 (21), 2109357.

Menon, G.K., Cleary, G.W., Lane, M.E., 2012. The structure and function of the stratum corneum. Int. J. Pharm. 435 (1), 3–9.

Murbach, M.D., Gerwe, B., Dawson-Elli, N., Tsui, L.-k., 2020. impedance. py: a Python package for electrochemical impedance analysis. J. Open Source Softw. 5 (52), 2349.

Nasrollaholhosseini, S.H., Mercier, J., Fischer, G., Besio, W.G., 2019. Electrode–electrolyte interface modeling and impedance characterizing of tripolar concentric ring electrode. IEEE (Inst. Electr. Electron. Eng.) Trans. Biomed. Eng. 66 (10), 2897–2905.

Sanei, S., Chambers, J.A., 2021. EEG Signal Processing and Machine Learning. John Wiley & Sons.

Shad, E.H.T., Molinas, M., Ytterdal, T., 2020. Impedance and noise of passive and active dry EEG electrodes: a review. IEEE Sensor. J. 20 (24), 14565–14577.

Strahl, S., Dhanasingh, A., Jolly, C., 2016. Cochlear implant electrode with liquid metal alloy. U.S. Patent 9,278,209, issued March 8, 2016.

Tang, S.-Y., Tabor, C., Kalantar-Zadeh, K., Dickey, M.D., 2021. Gallium liquid metal: the devil's elixir. Annu. Rev. Mater. Res. 51, 381–408.

Wang, D., Gao, C., Zhou, C., Lin, Z., He, Q., 2020. Leukocyte membrane-coated liquid metal nanoswimmers for actively targeted delivery and synergistic chemophotothermal therapy. Research 2020, 3676954.

Webster, J.G., 2009. Medical Instrumentation: Application and Design. John Wiley & Sons.

Yang, L., Li, H., Ding, J., Li, W., Dong, X., Wen, Z., Shi, X., 2018. Optimal combination of electrodes and conductive gels for brain electrical impedance tomography. Biomed. Eng. Online 17, 1–22.

Yu, Y., Zhang, J., Liu, J., 2013. Biomedical implementation of liquid metal ink as drawable ECG electrode and skin circuit. PLoS One 8 (3), e58771.

Zhang, C., Yang, B., Biazik, J.M., Webster, R.F., Xie, W., Tang, J., Allioux, F.-M., Abbasi, R., Mousavi, M., Goldys, E.M., 2022. Gallium nanodroplets are anti-inflammatory without interfering with iron homeostasis. ACS Nano 16 (6), 8891–8903.

Zhao, X., Zhou, Y., Xu, J., Chen, G., Fang, Y., Tat, T., Xiao, X., Song, Y., Li, S., Chen, J., 2021. Soft fibers with magnetoelasticity for wearable electronics. Nat. Commun. 12 (1), 6755.

Zhou, Y., Zhao, X., Xu, J., Fang, Y., Chen, G., Song, Y., Li, S., Chen, J., 2021. Giant magnetoelastic effect in soft systems for bioelectronics. Nat. Mater. 20 (12), 1670–1676.

Zhu, P., Gao, S., Lin, H., Lu, X., Yang, B., Zhang, L., Chen, Y., Shi, J., 2019. Inorganic nanoshell-stabilized liquid metal for targeted photonanomedicine in NIR-II biowindow. Nano Lett. 19 (3), 2128–2137.